Structure and Spectroelectrochemistry (UV/Vis, IR, EPR) of the Acceptor-Bridged Heterodinuclear Complex $[(\eta^5\text{-}C_5Me_5)ClRh(\mu\text{-bptz})Re(CO)_3Cl](PF_6)$, bptz = 3,6-Bis(2-pyridyl)-1,2,4,5-tetrazine

Thomas Scheiring,[†] Jan Fiedler,[‡] and Wolfgang Kaim*[,†]

Institut für Anorganische Chemie, Universität Stuttgart, Pfaffenwaldring 55, D-70550 Stuttgart, Germany, and J. Heyrovsky Institute of Physical Chemistry, Academy of Sciences of the Czech Republic, Dolejškova 3, CZ-18223 Prague, Czech Republic

Received October 17, 2000

The title complex contains two organometallic reaction centers which are known to engage in hydride transfer catalysis (Rh) or in CO_2 activation (Re), each after reductive elimination of the respective chloride ligand. The bridged heterodinuclear compound has been structurally characterized in the form where the chloride ligands are in *cis*-configuration relative to the bptz plane. The complex was subjected to cyclic voltammetry and spectroelectrochemical reduction to reveal an electrochemically reversible one-electron uptake by the bptz bridge, a rhodium chloride-dissociative second reduction to yield neutral $[(\eta^5\text{-}C_5Me_5)Rh(\mu\text{-bptz})Re(CO)_3\text{-}Cl]$, and a quasi-reversible third one-electron reduction.

Introduction

Heterodinuclear (heterobimetallic) complexes with two different functional metal centers are interesting as models for bimetallic catalysts.[1,2] In the following we describe a compound that contains two different chlorometal reaction centers, bridged by the strong π acceptor ligand 3,6-bis(2-pyridyl)-1,2,4,5-tetrazine (bptz), which has been shown to effectively mediate metal−metal interaction.[3−5]

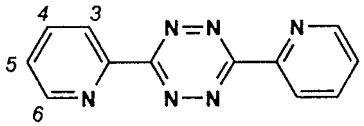

bptz

The coordinated metal complex fragments are (i) $[(\eta^5\text{-}C_5Me_5)ClRh]^+$, which is known as a center for hydride transfer catalysis after reductive activation of complexes with α-diimine ligands such as 2,2′-bipyridine,[6−8] and (ii) $[(OC)_3ClRe]$, which has been much studied with α-diimine ligands in the photo- and electrocatalytic reduction of CO_2 to CO.[9−11]

Coupling of both processes in a heterodinuclear arrangement to produce hydrogenated products of the CO_2 reduction would thus be an attractive approach.

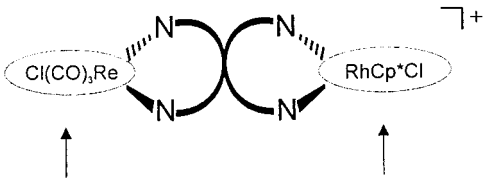

In this report we describe the synthesis of $[(\eta^5\text{-}C_5Me_5)ClRh(\mu\text{-bptz})Re(CO)_3Cl](PF_6)$ from the mononuclear precursor $(bptz)Re(CO)_3Cl$ and its crystal structure. Cyclic voltammetry and spectroelectrochemistry in the UV/vis and IR regions as well as EPR results are used to determine the sites of electron addition and the resulting effects in terms of chloride ligand labilization. Related previous studies have focused on the electronic coupling of electron transfer and/or bond-breaking processes via noninnocent bridging ligands in *homo*dinuclear complexes;[5,12−14] this is the first time that a *hetero*dinuclear system is the subject of such a detailed approach.

* To whom correspondence should be addressed. E-mail: kaim@iac.uni-stuttgart.de.
[†] Institut für Anorganische Chemie.
[‡] Heyrovsky Institute.

(1) George, S. M. *Chem. Rev.* **1995**, *95*, 475.
(2) Adams, R. D., Barnard, T. S.; Li, Z.; Wu, W.; Yamamoto, J. H. *J. Am. Chem. Soc.* **1994**, *116*, 9103.
(3) (a) Poppe, J.; Moscherosch, M.; Kaim, W. *Inorg. Chem.* **1993**, *32*, 2, 2640. (b) See also: Roche, S.; Thomas, J. A.; Yellowlees, L. J. *J. Chem. Soc., Chem. Commun.* **1998**, 1429.
(4) Gloeckle, M.; Fiedler, J.; Katz, N. E.; Garcia Posse, M.; Cutin, E.; Kaim, W. *Inorg. Chem.* **1999**, *38*, 3270.
(5) Kaim, W.; Reinhardt, R.; Fiedler, J. *Angew. Chem.* **1999**, *109*, 2600; *Angew. Chem., Int. Ed. Engl.* **1997**, *36*, 2493.
(6) Koelle, U.; Graetzel, M. *Angew. Chem.* **1987**, *99*, 572; *Angew. Chem., Int. Ed. Engl.* **1987**, *26*, 568.
(7) Cosnier, C.; Deronzier, A.; Vlachopoulos, N. *J. Chem. Soc., Chem. Commun.* **1989**, 1259.
(8) Ladwig, M.; Kaim, W. *J. Organomet. Chem.* **1991**, *419*, 233.
(9) Sullivan, B. P.; Meyer, T. J. *J. Chem. Soc., Chem. Commun.* **1984**, 1244.
(10) Hawecker, J.; Lehn, J. M.; Ziessel, R. *Helv. Chim. Acta* **1986**, *69*, 1900.
(11) (a) Christensen, P.; Hamnett, A.; Muir, A. V. G.; Timney, J. A. *J. Chem. Soc., Dalton Trans.* **1992**, 1455. (b) Johnson, F. P. A.; George, M. W.; Hartl, F.; Turner, J. J. *Organometallics* **1996**, *15*, 3374.
(12) Kaim, W.; Berger, S.; Greulich, S.; Reinhardt, R.; Fiedler, J *J. Organomet. Chem.* **1999**, *582*, 153.
(13) Baumann, F.; Stange, A.; Kaim, W. *Inorg. Chem. Commun.* **1998**, *1*, 305.
(14) (a) Berger, S.; Klein, A.; Wanner, M.; Fiedler, J.; Kaim, W. *Inorg. Chem.* **2000**, *39*, 2516. (b) Kaim, W.; Reinhardt, R.; Greulich, S.; Sieger, M.; Fiedler, J. *Collect. Czech. Chem. Commun.*, in press.

10.1021/om000892b CCC: $20.00
Publication on Web 03/09/2001

Experimental Section

Instrumentation. EPR spectra were recorded in the X band on a Bruker System ESP 300 equipped with a Bruker ER035M gaussmeter and a HP 5350B microwave counter. ^{1}H NMR spectra were taken on a Bruker AC 250 spectrometer, and infrared spectra were obtained using Perkin-Elmer Paragon 1000 and Phillips PU 9800 FTIR spectrometers. Absorption spectra were recorded on a Bruins Instruments Omega 10 spectrophotometer. Cyclic voltammetry was carried out at 100 mV/s standard scan rate in dichloromethane/0.1 M Bu_4NPF_6 using a three-electrode configuration (glassy carbon working electrode, Pt counter electrode, Ag/AgCl reference) and a PAR 273 potentiostat and function generator. The ferrocene/ferrocenium couple served as internal reference.[15a] The program DigiSim[15b] was used for graphical simulation. Spectroelectrochemical measurements were performed using an optically transparent thin-layer electrode (OTTLE) cell[16] for UV/vis spectra and a two-electrode capillary for EPR studies.[17]

(bptz)Re(CO)$_3$Cl. An amount of 76 mg (0.21 mmol) of Re(CO)$_5$Cl is heated to reflux with 49 mg (0.21 mmol) of bptz[16] in 30 mL of a toluene/dichloromethane mixture (3:1) for 40 min. After cooling to room temperature, the purplish red solution is concentrated to 20 mL, treated with 5 mL of pentane, and cooled to 0 °C overnight. The dark purple precipitate formed is collected, washed with diethyl ether, and dried in vacuo to yield 81 mg (71%). Anal. Calcd for $C_{15}H_8ClN_6O_3Re$ (541.9 g/mol): C, 33.25; H, 1.49; N, 15.51. Found: C, 33.07; H, 1.27; N, 15.21. ^{1}H NMR (CD_2Cl_2): δ 7.67 (ddd,1H, H$^{5'}$), 7.85 (ddd, 1H, H^5), 8.08 (td, 1H, H$^{4'}$), 8.32 (td, 1H, H^4), 8.73 (dt, 1H, H$^{3'}$), 9.02 (ddd, 1H, H^6), 9.06 (ddd, 1H, H^3), 9.11 (ddd, 1H, H^6) ppm. ^3J(H^{3}H^4) = 8.1 Hz, ^4J(H^{3}H^5) = 1.7 Hz, ^5J(H^{3}H^6) = 0.8 Hz, ^3J(H^{4}H^5) =7.9 Hz, ^4J(H^{4}H^6) = 1.6 Hz, ^3J(H^{5}H^6) = 5.3 Hz, ^3J(H$^{3'}$H$^{4'}$) = 8.1 Hz, ^4J(H$^{3'}$H$^{5'}$) = 1.1 Hz, ^3J(H$^{4'}$H$^{5'}$) = 7.9 Hz, ^4J(H$^{4'}$H$^{6'}$) = 1.5 Hz, ^3J(H$^{5'}$H$^{6'}$) = 4.8 Hz. UV/vis (CH_2Cl_2): λ_{max} (ϵ) 565 (6300), 505 (5240), 317 (29850) nm (M^{-1} cm^{-1}). IR (CH_2Cl_2): ν_{CO} 2032, 1946, 1919 cm^{-1}.

[(η^5-C$_5$Me$_5$)ClRh(μ-bptz)Re(CO)$_3$Cl](PF$_6$). An amount of 43 mg (0.07 mmol) of [Rh(C$_5$Me$_5$)Cl$_2$]$_2$ in 20 mL of acetone is stirred with 35 mg (0.14 mmol) of $AgPF_6$ for 30 min in the dark. The precipitate formed (AgCl) is removed through repeated filtration over Celite, and the orange-colored filtrate is then slowly added to 76 mg (0.14 mmol) of (bptz)Re(CO)$_3$Cl dissolved in 20 mL acetone. The blue solution obtained after stirring for 1 h at room temperature is concentrated to 10 mL, treated with 5 mL of pentane, and cooled to 0 °C. The blue precipitate formed is collected, washed with diethyl ether, and dried in vacuo to yield 115 mg (85%). Anal. Calcd for $C_{25}H_{23}Cl_2F_6N_6O_3PReRh$ (960.5 g/mol): C, 31.26; H, 2.41; N, 8.75. Found: C, 31.20; H, 2.38; N, 8.54. ^{1}H NMR (CD_2Cl_2): δ 1.95 and 1.98 (s, 15H, C$_5$Me$_5$), 7.91 (d, 1H, H$^{5'}$), 7.95 (d, 1H, H^5), 8.27 (t, 1H, H$^{4'}$), 8.42 (td, 1H, H^4), 8.93 (dt, 1H, H$^{3'}$), 9.06 (d, 1H, H^6), 9.08 (d, 1H, H^3), 9.31 (d, 1H, H$^{6'}$) ppm. ^3J(H^{3}H^4) = 8.0 Hz, ^3J(H^{4}H^5) = 7.9 Hz, ^3J(H^{5}H^6) = 5.1 Hz, ^3J(H$^{3'}$H$^{4'}$) = 7.9 Hz, ^3J(H$^{4'}$H$^{5'}$) = 8.2 Hz, ^3J(H$^{5'}$H$^{6'}$) = 4.9 Hz. UV/vis (CH_2Cl_2): λ_{max} (ϵ) 670 (10510), 315 (28200) nm (M^{-1} cm^{-1}). IR (CH_2Cl_2): ν_{CO} 2033, 1957, 1947 cm^{-1}.

Crystallography. Single crystals of [(η^5-C$_5$Me$_5$)ClRh(μ-bptz)Re(CO)$_3$Cl](PF$_6$) were obtained through slow diffusion of *n*-pentane into a saturated dichloromethane solution. Crystallographic and refinement information is summarized in Table 1. The structure was solved using the program SHELXTL 5.1,[18] and heavy atoms were located via the Patterson procedure. Non-hydrogen atoms were refined anisotropically, and hydrogen atoms were introduced at appropriate positions with coupled isotropic temperature factors.

Table 1. Crystal Data and Structure Refinement Information for [(η^5-C$_5$Me$_5$)ClRh(μ-bptz)Re(CO)$_3$Cl](PF$_6$)

formula	$C_{25}H_{23}Cl_2N_6O_3PReRh$
mol wt	960.47
temp, K	183
wavelength, Å	0.71073
cryst syst	orthorhombic
space group	*Pccn*
a, Å	19.826(4)
b, Å	23.561(5)
c, Å	15.598(3)
α, deg	90.00
β, deg	110.46(2)
γ, deg	90.00
volume, Å^3	7286.0(3)
Z	8
ρ(calcd), g cm^{-3}	1.751
absn coeff, mm^{-1}	4.028
F(000)	3696
cryst size, mm	0.3 × 0.2 × 0.2
2θ range, deg	1.73−26.00
index ranges	$-1 \le h \le 24$, $-1 \le k \le 29$, $-1 \le l \le 19$
no. of reflns measd	8564
no. of ind reflns	7156 [R(int) = 0.0575]
refinement method	full-matrix least-squares
no. of data/restraints/params	7156/0/396
goodness-of-fit on F^2	1.086
final R^a indices [$I > 2\sigma(I)$]	R1 = 0.0690, wR2 = 0.1528
R^a indices (all data)	R1 = 0.1304, wR2 = 0.1844
largest diff peak and hole, e Å^{-3}	2.174 and −2.375

^{a} R1 = $(\sum||F_o| - |F_c||)/\sum|F_o|$; wR2 = $\{\sum[w(|F_o|^2 - |F_c|^2)^2]/\sum[w(F_o^4)]\}^{1/2}$.

Results and Discussion

Synthesis. The mononuclear precursor (bptz)Re(CO)$_3$Cl was obtained by brief reaction of Re(CO)$_5$Cl with bptz in toluene/dichloromethane. Prolonged heating yielded the previously reported[19] dirhenium(I) compound. Mononuclear (bptz)Re(CO)$_3$Cl exhibits the typical response of (α-diimine)Re(CO)$_3$Cl complexes[19,20] on reduction, i.e., a reversible process, followed by an irreversible wave due to the rapid dissociation of chloride. EPR spectroscopy of [(bptz)Re(CO)$_3$Cl]$^{\bullet-}$ indicates bptz ligand-centered spin with g = 2.0038 and a(Re) = 1.62 mT.

Reaction of (bptz)Re(CO)$_3$Cl with [(η^5-C$_5$Me$_5$)RhCl$_2$]$_2$/$AgPF_6$ yielded blue [(η^5-C$_5$Me$_5$)ClRh(μ-bptz)Re(CO)$_3$Cl](PF$_6$). Attempts to start from a mononuclear rhodium(III) complex [(η^5-C$_5$Me$_5$)ClRh(bptz)](PF$_6$) and reacting this with Re(CO)$_5$Cl yielded only the dirhenium compound.[19]

Structure. The heterodinuclear [(η^5-C$_5$Me$_5$)ClRh(μ-bptz)Re(CO)$_3$Cl](PF$_6$) could be crystallized for structure analysis. Tables 1 and 2 summarize the results; Figure 1 illustrates the molecular structure.

The low symmetry of both coordinated metal complex fragments causes positional isomerism (*cis*/*trans*) with respect to the approximately planar bptz bridge (Scheme 1). ^{1}H NMR spectroscopy shows two isomers present in a 2:1 ratio. Figure 1 illustrates that in the isolated single

(15) (a) Connelly, N. G.; Geiger, W. E. *Chem. Rev.* **1996**, *96*, 877. (b) *DigiSim, version 2.1*; Bioanalytical Systems, BAS: West Lafayette, IN, 1996.
(16) Krejcik, M.; Danek, M.; Hartl, F. *J. Electroanal. Chem.* **1991**, *317*, 179.
(17) Kaim, W.; Ernst, S.; Kasack, V. *J. Am. Chem. Soc.* **1990**, *112*, 173.
(18) *SHELXTL 5.1*; Bruker Analytical X-ray Systems: Rheinstetten, Germany, 1998.
(19) Kaim, W.; Kohlmann, S. *Inorg. Chem.* **1990**, *29*, 2909.
(20) Klein, A.; Vogler, C.; Kaim, W. *Organometallics* **1996**, *15*, 236.

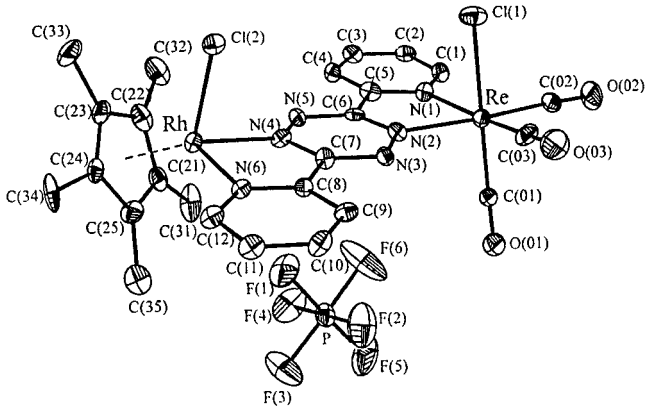

Figure 1. Molecular structure of $[(C_5Me_5)ClRh(\mu\text{-bptz})Re(CO)_3Cl](PF_6)$ in the crystal.

Scheme 1

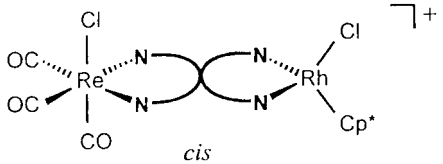

cis

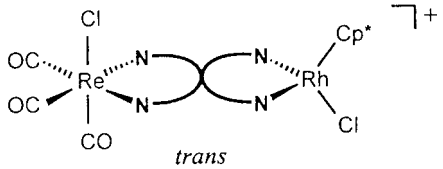

trans

Table 2. Selected Bond Lengths (Å) and Angles (deg) for $[(\eta^5\text{-}C_5Me_5)ClRh(\mu\text{-bptz})Re(CO)_3Cl](PF_6)$

Bond Lengths			
Re−C(01)	1.915(13)	N(4)−Rh	2.063(10)
Re−C(02)	1.937(14)	N(6)−Rh	2.142(10)
Re−C(03)	1.935(16)	N(2)−N(3)	1.318(13)
Re−N(1)	2.194(10)	N(4)−N(5)	1.317(13)
Re−N(2)	2.117(10)	N(2)−C(6)	1.337(15)
Re−Cl(1)	2.443(4)	N(3)−C(7)	1.348(15)
C(01)−O(01)	1.161(15)	N(4)−C(7)	1.350(15)
C(02)−O(02)	1.152(16)	N(5)−C(6)	1.364(15)
C(03)−O(03)	1.149(18)	C(5)−C(6)	1.464(15)
Rh−Cl(2)	2.392(3)	C(7)−C(8)	1.482(15)
Rh−C(21)	2.164(13)		
Rh−C(22)	2.125(14)		
Rh−C(23)	2.172(13)		
Rh−C(24)	2.175(13)		
Rh−C(25)	2.157(14)		

Bond Angles			
C(01)−Re−C(02)	87.5(6)	O(01)−C(01)−Re	177.2(11)
C(01)−Re−C(03)	90.8(6)	O(02)−C(02)−Re	177.0(14)
C(03)−Re−C(02)	90.2(6)	O(03)−C(03)−Re	177.7(13)
C(01)−Re−N(2)	94.0(5)	C(5)−N(1)−Re	116.2(8)
C(02)−Re−N(2)	173.0(5)	C(6)−N(2)−Re	116.2(8)
C(03)−Re−N(2)	96.6(5)	N(4)−Rh−Cl(2)	85.9(3)
C(01)−Re−N(1)	97.2(5)	N(6)−Rh−Cl(2)	86.0(3)
C(02)−Re−N(1)	97.6(5)	C(7)−N(4)−Rh	117.2(8)
C(03)−Re−N(1)	169.0(5)	C(8)−N(6)−Rh	115.9(8)
N(2)−Re−N(1)	75.4(4)	N(4)−Rh−N(6)	76.6(4)
C(01)−Re−Cl(1)	178.6(4)	N(1)−C(5)−C(6)	113.3(11)
C(03)−Re−Cl(1)	87.8(4)	N(6)−C(8)−C(7)	114.5(10)
C(02)−Re−Cl(1)	93.0(4)	N(4)−C(7)−C(8)	115.2(11)
N(2)−Re−Cl(1)	85.7(3)	N(2)−C(6)−C(5)	118.6(11)
N(1)−Re−Cl(1)	84.2(3)		

crystal the chloride ligands are in a *cis* position relative to the bptz ligand plane, the dihedral angles between 2-pyridyl and tetrazine rings being smaller than 2°.

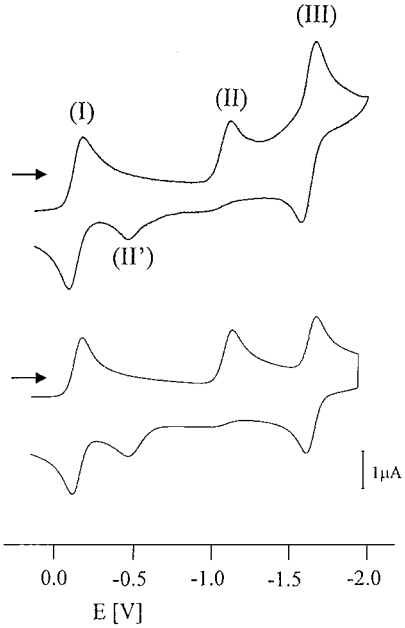

Figure 2. Cyclic voltammogram of $[(C_5Me_5)ClRh(\mu\text{-bptz})Re(CO)_3Cl](PF_6)$ in CH_2Cl_2/0.1 M Bu_4NPF_6 at 100 mV/s scan rate (top) with graphical simulation (bottom, cf. Table 3). Potentials in V vs $[Fe(C_5H_5)_2]^{+/0}$.

Contact with the PF_6^- counterion appears to relate to the slight displacement of both metal centers out of the bptz plane. The dihedral angles between the N−M−N planes and the bptz best plane are 5.9° for rhodium and 4.6° for rhenium. As a consequence of these slight tilts toward the "chloride side", the intramolecular Cl−Cl distance is smaller at 6.24 Å than the Re−Rh distance of 6.865 Å.

The metal−N(bptz) bonds show a characteristic variation: The longest bond at 2.194(10) Å is that between rhenium(I) and the corresponding pyridyl nitrogen atom. The bond to the much better π-accepting tetrazine nitrogen center is shorter at 2.117(10) Å, and the Re^{I}−bptz π back-donation makes the tetrazine ring sufficiently electron rich to allow for a rather short bond of 2.063(10) Å between cationic rhodium(III) and the corresponding tetrazine nitrogen center. At 2.142(10) Å the Rh^{III}−N(pyridine) bond has an intermediate length.

The rhenium(I) center has the expected[21] approximately octahedral configuration, while the other d^6 metal center, rhodium(III), similarly exhibits two almost right angles, N−Rh−Cl at 85.9(3)° and 86.0(3)°. The dihedral angle between C_5Me_5 and the bptz ligand is 65.4(3)°. The bite angles of 75.4(4)° at rhenium(I) and of 76.6(4)° at rhodium(III) are comparable.

The distances within the tetrazine ring do not indicate major electron transfer from the metal complex fragments to the bptz ligand; the N−N bonds of about 1.32 Å and the C−N bonds of about 1.35 Å are typical for nonreduced tetrazines.[22] In contrast, a recently reported structure of $[(Ph_3P)_2Cu(\mu\text{-bptz})Cu(PPh_3)_2](BF_4)$ with the $bptz^{\bullet-}$ anion radical ligand showed lengthened N−N and slightly shortened C−N bonds.[23]

(21) Hartmann, H., Scheiring, T.; Fiedler, J.; Kaim, W. *J. Organomet. Chem.* **2000**, *604*, 267.
(22) Campos-Fernández, C. S.; Clérac, R.; Dunbar, K. R. *Angew. Chem.* **1999**, *111*, 3685; *Angew. Chem., Int. Ed.* **1999**, *38*, 3477.
(23) Schwach, M.; Hausen, H.-D.; Kaim, W. *Inorg. Chem.* **1999**, *38*, 2242.

Table 3. Electrochemical Data[a] of Complexes

complex	$E_{1/2}$(I)	E_{pc}(II)	E_{pa}(II′)	$E_{1/2}$(III)	solvent	ref
(bptz)Re(CO)$_3$Cl	−0.72	−1.97			CH_2Cl_2	*b*
[(C$_5$Me$_5$)ClRh(μ-bptz)Re(CO)$_3$Cl](PF$_6$)[c]	−0.18	−1.14	−0.47	−1.61	CH_2Cl_2	*b*
[(C$_5$Me$_5$)ClRh(μ-bptz)Rh(C$_5$Me$_5$)Cl](PF$_6$)$_2$	0.00	−1.06	−0.46	−1.37[d]	CH_3CN	5
(CO)$_3$ClRe(μ-bptz)Re(CO)$_3$Cl	−0.12	−1.45			DCE	19

[a] From cyclic voltammetry at 100 mV/s in 0.1 M Bu_4NPF_6 solutions. Potentials in V vs $[Fe(C_5H_5)_2]^{+/0}$. [b] This work. [c] Simulation parameters (Figure 2): k_s values at 200 (I), 0.008 (II), 0.0022 (II′), and 1 cm s^{-1} (III); $E_{1/2} = -0.57$ V for reoxidation of (C$_5$Me$_5$)Rh(μ-bptz)Re(CO)$_3$Cl; $E_{1/2} = -1.12$ V for $E_{1/2}$ (II). [d] Peak potential for irreversible process.

Table 4. UV/Vis Absorption and IR Vibrational Data[a]

compound	λ_{max} [nm] ($\epsilon \times 10^{-3}$ [M^{-1} cm^{-1}])	ν_{CO} [cm^{-1}]
(bptz)Re(CO)$_3$Cl	565 (6.30), 505sh, 317 (29.9)	2032, 1946, 1919
[(bptz)Re(CO)$_3$Cl]$^{\bullet-}$	390 (5.10), 295 (24.8)	2013, 1907, 1881
[(C$_5$Me$_5$)ClRh(μ-bptz)Re(CO)$_3$Cl]$^+$	670 (10.5), 505sh, 315 (28.2)	2033, 1957, 1947
[(C$_5$Me$_5$)ClRh(μ-bptz)Re(CO)$_3$Cl]$^{\bullet}$	468 (6.2), 368sh, 295 (20.2)	2017, 1917, 1891
(C$_5$Me$_5$)Rh(μ-bptz)Re(CO)$_3$Cl	643 (17.8), 482 (6.2), 295 (20.2)	2015, 1912, 1884
[(C$_5$Me$_5$)Rh(μ-bptz)Re(CO)$_3$]$^{\bullet}$	395sh	*b*

[a] From spectroelectrochemistry in CH_2Cl_2/0.1 M Bu_4NPF_6. [b] Not recorded.

Cyclic Voltammetry and Spectroelectrochemistry. The (spectro)electrochemical studies decribed in the following were performed with the isomer mixture as obtained in the preparation. Previous studies have shown little effect of such positional isomerism on the potentials and spectral features,[5,12] wave splitting or line broadening was not observed here.

Cyclic voltammetry of [(η^5-C$_5$Me$_5$)ClRh(μ-bptz)Re(CO)$_3$Cl](PF$_6$) in CH_2Cl_2/0.1 M Bu_4NPF_6 reveals a particular sequence (Figure 2). The first reversible one-electron reduction at the expected[5,19] positive value is followed by an irreversible second wave. This cathodic signal has a corresponding anodic counter peak at an anodically shifted potential, a response that is a familiar[6−8] EEC or ECE feature for α-diimine complexes with [(η^5-C$_5$Me$_5$)ClRh]$^+$ but not for Re(CO)$_3$Cl compounds with such ligands.[19−21] (E: electron transfer step; C: chemical step, e.g., atom dissociation.) At still more negative potentials, a cyclovoltammetrically reversible third one-electron reduction is observed (Figure 2); the data are summarized in Table 3.

The interpretation of the cyclic voltammetric response relies on information from spectroelectrochemistry in the UV/vis and IR regions (Table 4) and on EPR spectroscopy of the first reduced state. The EPR spectrum of [(C$_5$Me$_5$)ClRh(μ-bptz)Re(CO)$_3$Cl]$^{\bullet}$ in CH_2Cl_2/0.1 M Bu_4NPF_6 shows the typical "two-line" pattern[19,20] from an only partially resolved sextet which is due to the coupling of the electron spin with one rhenium center (^{185}Re: I = 5:2, 37.4%; ^{187}Re, I = 5:2, 62.6%). Both the relatively[19,20,24] small metal coupling constant of 2.0 mT and the *g* factor of 2.0025 very close to the free electron value of 2.0023 indicate the occupation of a bptz ligand-based MO on one-electron reduction.[25] The radical complexes [(C$_5$Me$_5$)ClRh(μ-bptz)Re(CO)$_3$Cl]$^{\bullet}$ and [(bptz)-Re(CO)$_3$Cl]$^{\bullet-}$ exhibit rather similar *a* and *g* values, suggesting little perturbation of the singly occupied molecular orbital by the additionally coordinated complex fragment [(C$_5$Me$_5$)ClRh]$^+$.

UV/vis spectroelectrochemistry in dichloromethane (Figure 3, Table 4), using an optically transparent thin-layer electrolytic (OTTLE) cell,[14] supports this interpretation. The intense rhenium metal-to-bptz ligand charge transfer band at 670 nm is hypsochromically shifted to 469 nm and reduced in intensity, in agreement with a singly occupied orbital π^*(bptz). Apparently, the bptz radical anion exhibits only weak intraligand transitions in the visible. The result of the second, irreversible electron addition is the emergence of an intense and rather narrow ($\Delta\nu = 1900$ cm^{-1}) band at

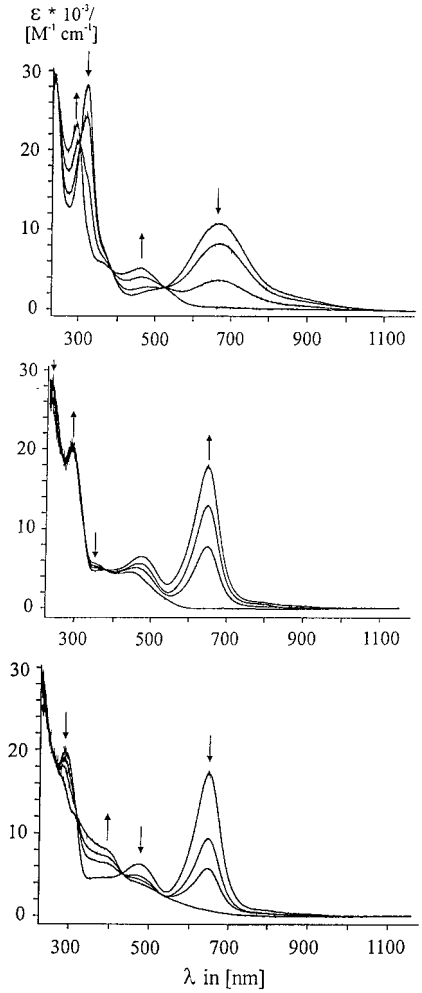

Figure 3. Successive UV/vis spectroelectrochemistry of [(C$_5$Me$_5$)ClRh(μ-bptz)Re(CO)$_3$Cl](PF$_6$) in CH_2Cl_2/0.1 M Bu_4NPF_6 (cf. Scheme 3).

(24) Isotropic hyperfine values a_o: Weil, J. A.; Bolton, J. R.; Wertz, J. E. *Electron Paramagnetic Resonance*; Wiley: New York, 1994.
(25) Kaim, W. *Coord. Chem. Rev.* **1987**, *76*, 187.

Scheme 2

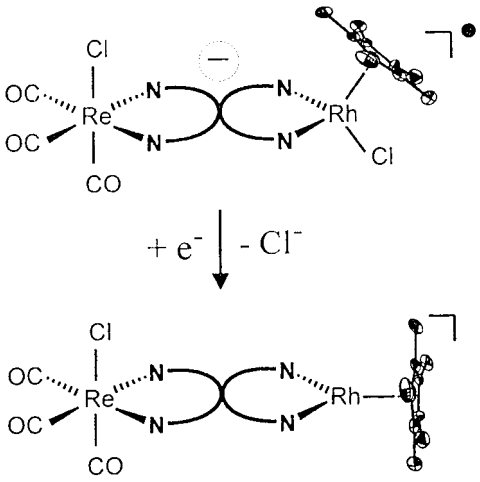

Scheme 3

$[(\eta^5\text{-}C_5Me_5)ClRh(\mu\text{-bptz})Re(CO)_3Cl]^+$

E(I) ↑↓ E

$[(\eta^5\text{-}C_5Me_5)ClRh(\mu\text{-bptz})Re(CO)_3Cl]^\bullet$

E(II) ↑↓ EC

$(\eta^5\text{-}C_5Me_5)Rh(\mu\text{-bptz})Re(CO)_3Cl + Cl^-$

E(III) ↑↓ E

$[(\eta^5\text{-}C_5Me_5)Rh(\mu\text{-bptz})Re(CO)_3Cl]^{\bullet-}$

$-Cl^-$ ↓ C (slow)

$[(\eta^5\text{-}C_5Me_5)Rh(\mu\text{-bptz})Re(CO)_3]^\bullet$

643 nm, very typical[5,8] for the long-wavelength transitions between two molecular orbitals containing strongly mixed α-diimine π^* and d_π components.[26] Comparison with data for the homodinuclear systems $[Cl(OC)_3Re(\mu\text{-bptz})Re(CO)_3Cl]$[19,21] and $[(C_5Me_5)ClRh(\mu\text{-bptz})RhCl(C_5Me_5)](PF_6)_2$[5] supports these assignments.

We thus invoke an overall two-electron reductive chloride dissociation from the rhodium(III) center via the one-electron reduced ("electron reservoir"[5]) radical intermediate to produce formally a neutral rhenium(I)−rhodium(I) species $[(\eta^5\text{-}C_5Me_5)Rh(\mu\text{-bptz})Re(CO)_3Cl]$ (Scheme 2). On the addition of a third electron, the intense long-wavelength band disappears (Figure 3) and a slow, irreversible loss of the chloride bound to rhenium occurs (Scheme 3).

Spectroelectrochemistry in the carbonyl stretching region of the IR shows a typical[11,20,21,27] low-energy shift on the first reduction but only a very small such shift after the chloride-dissociative second reduction (Figure 4, Table 4). Apparently, the response at the tricarbonylrhenium fragment is very much determined by the charge which changes during the first but not during the second reduction (Scheme 3). The crucial role of the charge for metal carbonyl stretching frequencies has been noted previously for molybdenum carbonyl compounds where ligand- and metal-based electron transfer caused surprisingly similar shifts in ν(CO).[28]

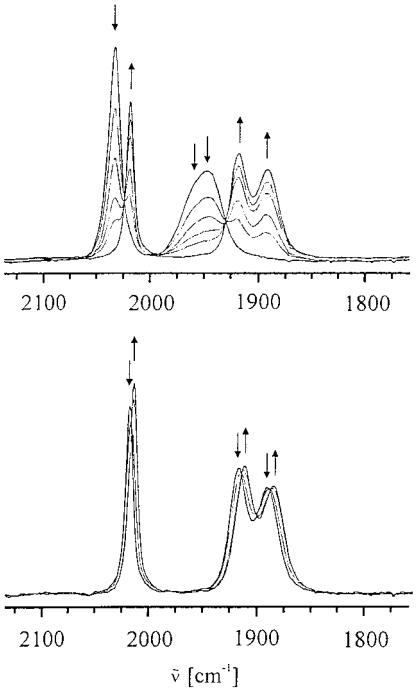

Figure 4. Successive IR spectroelectrochemistry of $[(C_5Me_5)ClRh(\mu\text{-bptz})Re(CO)_3Cl](PF_6)$ in CH_2Cl_2/0.1 M Bu_4NPF_6 (cf. Scheme 3).

Summarizing, the heterodinuclear system studied shows two separated chloride dissociation steps, the first (after electron reservoir function of the bridging ligand) from the higher valent pentamethylcyclopentadienylrhodium(III) center and the second from the carbonylrhenium(I) moiety (Scheme 3). Future studies will have to show if both hydride formation and CO_2 coordination occur after sequential reductive dehalogenation and whether both activated components can be brought to reaction.

Acknowledgment. This work was supported by the Deutsche Forschungsgemeinschaft (SFB 270) and by the COST D14 program.

Supporting Information Available: Tables of X-ray crystallographic data for $[(\eta^5\text{-}C_5Me_5)ClRh(\mu\text{-bptz})Re(CO)_3Cl](PF_6)$ and a data sheet for the graphical simulation of the cyclic voltammogram. This material is available free of charge via the Internet at http://pubs.acs.org.

OM000892B

(26) Kaim, W.; Reinhardt, R.; Sieger, M. *Inorg. Chem.* **1994**, *33*, 4453.
(27) Stor, G. J.; Hartl, F.; van Outersterp, J. W. M.; Stufkens, D. J. *Organometallics* **1995**, *14*, 1115.
(28) Kaim, W.; Bruns, W.; Kohlmann, S.; Krejcik, M. *Inorg. Chim. Acta* **1995**, *229*, 143.